



CrossMark
click for updates

Research

Cite this article: Bartholomäus A, Fedyunin I, Feist P, Sin C, Zhang G, Valleriani A, Ignatova Z.

2016 Bacteria differently regulate mRNA abundance to specifically respond to various stresses. *Phil. Trans. R. Soc. A* **374**: 20150069. <http://dx.doi.org/10.1098/rsta.2015.0069>

Accepted: 29 June 2015

One contribution of 21 to a theme issue
'DNA as information'.

Subject Areas:

biochemistry, chemical biology,
computational chemistry

Keywords:

transcription, translation, deep sequencing,
Escherichia coli, copy numbers

Author for correspondence:

Zoya Ignatova
e-mail: zoya.ignatova@uni-hamburg.de

[†]These authors contributed equally to this study.

[‡]Present address: Institute of Life and Health Engineering, Jinan University, Guangzhou, China.

Electronic supplementary material is available at <http://dx.doi.org/10.1098/rsta.2015.0069> or via <http://rsta.royalsocietypublishing.org>.

Bacteria differently regulate mRNA abundance to specifically respond to various stresses

Alexander Bartholomäus^{1,2,†}, Ivan Fedyunin^{1,†}, Peter Feist¹, Celine Sin³, Gong Zhang^{1,‡}, Angelo Valleriani³ and Zoya Ignatova^{1,2}

¹Department of Biochemistry, University of Potsdam, Karl-Liebknecht-Straße 24-25, Potsdam 14476, Germany

²Institute for Biochemistry and Molecular Biology, Department of Chemistry, University of Hamburg, Martin-Luther-King-Platz 6, Hamburg 20146, Germany

³Department of Theory and Bio-Systems, Max Planck Institute of Colloids and Interfaces, Potsdam 14476, Germany

Environmental stress is detrimental to cell viability and requires an adequate reprogramming of cellular activities to maximize cell survival. We present a global analysis of the response of *Escherichia coli* to acute heat and osmotic stress. We combine deep sequencing of total mRNA and ribosome-protected fragments to provide a genome-wide map of the stress response at transcriptional and translational levels. For each type of stress, we observe a unique subset of genes that shape the stress-specific response. Upon temperature upshift, mRNAs with reduced folding stability up- and downstream of the start codon, and thus with more accessible initiation regions, are translationally favoured. Conversely, osmotic upshift causes a global reduction of highly translated transcripts with high copy numbers, allowing reallocation of translation resources to not degraded and newly synthesized mRNAs.

1. Introduction

Environmental stress and suboptimal growth conditions reduce cell viability and put cells at risk. Acute stress requires an immediate but specific response in order

to maximize cell survival. Multicellular organisms can efficiently buffer external changes using the capacity of internal homeostasis [1]. By contrast, unicellular organisms are directly exposed to sudden alterations of their environment and need to immediately reprogramme their cellular activities. By examining the gene expression of cells exposed to different types of stress numerous previous studies suggest that bacteria respond to stress over different time scales [2–5]. Gene expression is subject to extensive regulation at different levels, including transcription, mRNA degradation, translation and protein degradation. It is now clear that in each of these processes a series of regulatory steps is involved [6–9], but little is known about how their combined effect shapes the cellular response to stress in bacteria.

Advances in massively parallel nucleotide sequencing platforms and approaches to capture ribosomal position with nucleotide resolution [10] allow precise deconvolution of the control mechanisms of gene expression at translational level. This approach has been pioneered for yeast [10] and applied to bacteria to determine mRNA sequence features leading to non-uniform distribution of the ribosomal reads [11] and to monitor the co-translational binding of chaperones [12]. Here we modified this methodology and combined it with RNA-sequencing (RNA-Seq) to quantitatively assess transcriptional and translational response of *Escherichia coli* to different nutrient conditions and to acute heat and osmotic stress. Our analysis unravelled common and stress-specific response programmes which *E. coli* uses to counteract acute stress. In both types of stress, we observed that for a large fraction of genes changes in mRNA levels are co-directional with changes in translation. However, for each stress type, a significant group of genes opposed this trend and showed mainly translational regulation with no changes in the mRNA levels. Analysis of these gene subsets revealed disparate mode of translational regulation at each type of stress.

2. Material and methods

(a) Media, cultivation conditions and cell quantification

Escherichia coli MC4100 strain was cultured at 37°C to mid-log phase ($OD_{600} \sim 0.3$ or 0.4) in LB medium or MM medium ($12.8 \text{ g l}^{-1} \text{ Na}_2\text{HPO}_4 \times 7\text{H}_2\text{O}$, $3 \text{ g l}^{-1} \text{ KH}_2\text{PO}_4$, $1 \text{ g l}^{-1} \text{ NH}_4\text{Cl}$, 2 mM MgSO_4 , 0.1 mM CaCl_2 , 0.4% glucose). For heat stress, an aliquot of cells grown in LB medium was centrifuged for 4 min at $4000g$ at room temperature, resuspended in LB medium preheated to 47°C and further incubated for 7 min at 47°C. Osmotic stress was exerted to an aliquot of cells grown in MM medium by adding NaCl to 0.3 M (0.6 Osm) and further incubated for 20 min at 37°C. The number of viable cells was determined after staining the cells with BDTM Cell Viability Kit with liquid counting beads (BD Biosciences) and analysed by flow cytometry on a FACSCalibur (BD Biosciences) equipped with argon 488 nm and diode 632 nm lasers. The data were analysed with Cyfoogic v. 1.2.1 (CyFlo Ltd).

(b) Cell lysis, polysome isolation and enrichment of ribosome-protected fragments

To isolate mRNA-bound ribosome complexes we used a previously described approach [13] with some modifications. Exponentially growing cells were poured over crushed ice containing $100 \mu\text{g ml}^{-1}$ chloramphenicol and harvested by centrifugation at $5000g$ for 5 min at 4°C. All subsequent operations were carried out on ice with pre-chilled buffers. To obtain polysomal profiles, the cell pellet from 100 ml culture was resuspended in 12 ml of ice-cold sucrose-buffer solution ($16 \text{ mM Tris pH } 8.1$ supplemented with $0.5 \text{ M RNase-free sucrose}$, 50 mM KCl , 8.75 mM EDTA , $100 \mu\text{g ml}^{-1}$ chloramphenicol, $1.25 \text{ mg/ml lysozyme}$) and gently stirred for 5 min on ice. 0.3 ml of 1 M MgCl_2 was added to inhibit lysozyme and the suspension was spun at $6000g$ for 10 min at 4°C. The pellet was resuspended in 0.7 ml freshly prepared lysis buffer ($10 \text{ mM Tris pH } 7.8$ containing $50 \text{ mM NH}_4\text{Cl}$, 0.01 M MgCl_2 , 0.2% triton X-100, $100 \mu\text{g ml}^{-1}$ chloramphenicol and 10 U DNase I (RNase-free, Fermentas)). The lysate was clarified by centrifugation at $10\,000g$ for 10 min at 4°C and frozen at -80°C if not analysed immediately. Up to 0.4 ml of clarified lysate was

layered onto 15 to 50% (w/v) sucrose gradient (buffered in 10 mM Tris pH 7.8 supplemented with 50 mM NH_4Cl , 10 mM MgCl_2 , 0.2% triton X-100, 100 $\mu\text{g ml}^{-1}$ chloramphenicol) and centrifuged for 1.5 h at 35 000 r.p.m. in SW 55Ti rotor (Beckman) at 4°C. The gradient was slowly pumped out from the bottom of the tubes with a flow rate set to 0.38 ml min⁻¹ and the absorbance at 254 nm (A_{254}) was recorded via a flow-through UV spectrophotometer cell (Pharmacia LKB-UV-M II).

For the isolation of ribosome-protected fragments (RPFs), an aliquot of 100 A_{260} units of ribosome-bound mRNA fraction (prior to ultracentrifugation in the sucrose gradients, see above) was subjected to nucleolytic digestion with 10 units μl^{-1} micrococcal nuclease (Fermentas) for 10 min at room temperature in buffer of pH 9.2 (10 mM Tris pH 11 containing 50 mM NH_4Cl , 10 mM MgCl_2 , 0.2% triton X-100, 100 $\mu\text{g ml}^{-1}$ chloramphenicol and 20 mM CaCl_2). The monosomal fraction was separated by sucrose density gradient (15–50% w/v). The total RNA was isolated from the monosomes using the hot SDS/phenol method. The micrococcal nuclease also cleaved the rRNAs into fragments with a size similar to the RPFs. The sample was enriched predominantly in one rRNA fragment which was removed by subtractive hybridization at 70°C using a 5'-biotin-5'-GCCTCGTCATCACGCCCTCAGCC-3' DNA oligonucleotide along with μMACS Streptavidin Kit (Myltenyi Biotec) to remove the biotin-labelled DNA/rRNA hybrids. 3' Adapter was first ligated to the dephosphorylated fragments with T4 RNA ligase 2 truncated (New England Biolabs). Following 3' phosphorylation of the 5' adapter with T4 PNK (New England Biolabs), the 5' adapter was ligated to the fragment with T4 RNA ligase 2 truncated (New England Biolabs). The generation of the libraries was performed as described in [14].

(c) Random mRNA fragmentation and spike-in with a control RNA

Total RNA was isolated from approximately 6 ml exponentially growing bacteria with GeneJET™ RNAPurification Kit (Fermentas). Prokaryotic mRNA is a minor fraction of the total cellular RNA, therefore, mRNAs were enriched by removal of 16S and 23S rRNAs [15] with a MICROBExpress™ Bacterial mRNA Enrichment Kit (Ambion). Twenty microlitres of the enriched mRNA was mixed with equal volume of 2× alkaline fragmentation solution (2 mM EDTA and 100 mM Na_2CO_3 pH 9.2) and incubated for 40 min at 95°C. The reaction was stopped by adding 560 μl 300 mM NaOAc pH 5.5, followed by isopropanol precipitation [16]. For quantification [17], after the random fragmentation the RNA sample was spiked with an external 25-nt RNA standard (5'-AAUGAUAAUUCAAGAAUCAUAACGG-3') which does not align anywhere in the *E. coli* genome. Typically, 10 ng of spike-in RNA were added to 25.5 μg total extracted RNA. The optimal time for fragmentation of the mRNA was determined using GAPDH mRNA (0.25 μg ; Fermentas) and the spectra were recorded with BioAnalyzer (Agilent RNA 6000 Kit). RNA size selection and generation of the cDNA libraries was performed as described in [14].

(d) Mapping of the sequencing reads

Sequencing reads were aligned to *E. coli* K-12 substrain MG1655 genome sequence (GenBank: U00096.2) with FANSe mapping algorithm allowing up to three mismatches and enabled indel detection [18]. Note that the *E. coli* MC4100 genome differs from that of MG1655 by deletion of approximately 120 genes. The reads aligning to rRNA and tRNA genes were subtracted from the datasets. Sequencing reads spanning two (overlapping) open-reading frames (ORFs) were assigned to one of the two annotated ORFs (NCBI) based on the position of the middle nucleotide (nt). (For reads with an even number of nt-s, the nt closer to the 5'-terminus was arbitrarily taken as a middle nt.)

(e) Quantitative RT-PCR

Total mRNA was extracted using the GeneJET™ RNA Purification Kit (Fermentas) and treated with DNase I (Fermentas). The cDNA was synthesized with RevertAid™ H Minus Reverse

Transcriptase (Fermentas) and quantitative RT-PCR was performed on a StepOnePlus™ real-time PCR system (Applied Biosystems) using template-specific primers. The values were normalized to the amount of the total RNA.

(f) Quantification of the absolute transcript numbers

The copy number of the transcripts (X_i) was quantified using the following method [19]:

$$X_i = \frac{C_i}{CL_i} T, \quad (2.1)$$

where C_i represents the mapped reads on a transcript i with a length L_i (in nt), $C = \sum_i C_i$ is the sum of all mapped reads within a RNA-Seq dataset, whereas T is the length of the transcriptome in base pairs [19]. From the reads and the amount of the added spike-in standard, we determined the number of molecules of spike-in standard in nt. T was calculated by converting the total mRNA mapped reads in each RNA-Seq experiment into molecules of mRNA (in nt) using the number of molecules of spike-in standard (nt) and normalized per cell number quantified by fluorescence activated cell sorting (FACS).

The length of the transcriptome, T , in base pairs, is calculated as follows:

- (i) The amount (nanograms) of added spike-in standard was converted into molecules spike-in in nt using the molecular weight and nucleotide length of the spike-in and the Avogadro number.
- (ii) The total amount of mRNA to which the spike-in was added was converted into nt using the molecules of spike-in (nt) and the sequencing reads mapped to the transcriptome and spike-in standard.
- (iii) The total mRNA length (nt) was divided by the cell number quantified by FACS to calculate the total length (T) of the transcriptome per cell. $1.81 \times 10^8 \pm 2.4 \times 10^7$, $7.84 \times 10^8 \pm 1.21 \times 10^7$, $1.52 \times 10^8 \pm 2 \times 10^7$ and $4.72 \times 10^8 \pm 7.3 \times 10^7$ was the total number of cells in LB, MM, under heat or osmotic stress, respectively.
- (iv) Finally, to calculate the copy number of each gene, we multiply the rpkMd values of each gene C_i/CL by T (equation (2.1)).

(g) Differential gene expression and GO analyses

The number of raw reads unambiguously aligned to ORFs in both RNA-Seq and RPF datasets, for each condition, were normalized by the median of the total number of reads aligned to all ORFs, which gives more stable normalization [20] and is more suitable for differential expression analysis than other normalization approaches using total number of reads aligned to all ORFs (reads per total mapped reads, rpM, or fragment per total mapped reads, FPM) [21]. For comparison between different genes, the number of the aligned reads was normalized by the length of the ORF and the median of the total number of reads aligned to all ORFs (reads per kilobase of ORF per median of the total mapped reads, rpkMd). Furthermore, to avoid false-positives originating from genes with very low read counts, genes with mRNA or RPF read counts less than 60 were 'upgraded' to 60 in the differential gene expression analysis. The value of minimal 60 reads in both RNA-Seq and RPF-Seq analysis was determined from the analysis of the sampling error between two biological replicates as described [10]. Thereafter, the ribosome density (RD) for each gene was calculated as follows (note that it is similar to the definition of the TE value as described already [10]):

$$RD_i = \frac{RPF_i[rpMd]}{mRNA_i[rpMd]}. \quad (2.2)$$

To assess the biological functions affected by different stress conditions, we identified the GO terms with significant enrichment for each differentially expressed gene set using R (v. 2.15.2) and

Bioconductor packages *ecoli2.db* and *GO.db*. *p*-values were adjusted for multiple testing using false discovery rate (FDR) according to Benjamini & Hochberg [22].

(h) Secondary structure analysis

Structure profiles were computed with *RNAfold* program with default parameters from the *Vienna RNA Package 2.0* [23] using a sliding window with different widths reported in the literature for such analysis. For each nucleotide of a transcript the minimum free energy was calculated moving the window with a single nucleotide at a time. Average profiles for groups of genes were generated by taking the mean of their per-base folding energy contributions. The 23-nt window, with a width equal to the average of our read lengths, revealed very noisy profiles due to the small window size. By contrast, the 101-nt window, albeit informative on long-range interactions, smoothed too many features in the profiles. For our analysis, we chose the 39-nt window [24] which gave very similar result to the 51-bp window [25]. The significance of the structural differences between two gene groups was evaluated nucleotide-wise using a two-sample Kolmogorov–Smirnov test. A two-sided test was performed for each base and the corresponding *p*-values were collected and adjusted for multiple testing using FDR according to Benjamini & Hochberg [22]. To judge the significance of the whole curve, the single *p*-values were median averaged. We further assessed the uniqueness of the identified groups of genes by comparing the folding energy distributions to those of equally-sized random sets of genes. We analysed 10 000 subsamples with sample size equal to the gene group of interest and calculated a *p*-value as the number of points crossing the corresponding average folding profile divided by the total number of sampled points. The dispersion of the subsamples between 2.5th and 97.5th percentiles of the distribution of values per nt is shadowed grey (figure 4*b,d*).

3. Results

(a) Difference in gene expression between growth in mineral and complex media

We first compared the transcriptional and translational activities of *E. coli* (strain MC4100) at rapid growth in complex (LB) medium or at moderate growth rate in medium containing mineral compounds and glucose as the only carbon and energy source (minimal medium, MM). For both conditions we performed deep sequencing of the total mRNA (RNA-Seq) [19] and ribosome-protected fragments (RPF or RPF-Seq [14,16]) (figure 1*a*). The total mRNA was isolated from each sample and randomly fragmented under alkaline conditions into fragments with similar length to the RPFs (electronic supplementary material, figure S1*a*). We directly ligated 5'- and 3'-adapters to the RPFs and mRNA fragments which enabled us to capture transcripts of high and moderate abundance as well as low-abundance transcripts (figure 1*b*) with high reproducibility between biological replicates (electronic supplementary material, figure S1*b,c*). For each sequencing set, the unambiguously mapped mRNA and RPF reads were normalized by the median of the total number of reads mapped to all ORFs and presented as reads per median of the total mapped reads (rpMd) or reads per kilobase of ORF per median of the total mapped reads (rpKMd). Normalization by the median of the total number of reads aligned to all ORFs gives more stable normalization than normalization to reads per total mapped reads, rpM, or fragment per total mapped reads, FPM [20]. We spiked each RNA-Seq experiment (figure 1*a*) with an external RNA standard whose sequence does not align anywhere in the *E. coli* genome. Reads mapped to the spike in sequence showed high reproducibility between biological replicates. With this twist, the RNA-Seq datasets, normalized to the living cell counts (determined by FACS) were used to calculate the absolute copy number of each mRNA per cell (equation (2.1)). We were able to map reads to 4254 ORFs in LB and 4269 ORFs in MM. (In *E. coli*, the total number of genes including rRNA, tRNA and non-coding RNAs is 4496.)

Cells grown in LB medium have about three times more mRNA transcripts than cells grown in MM (approx. 7800 mRNA copies/cell versus approx. 2400 mRNA copies/cell; figure 1*b*);

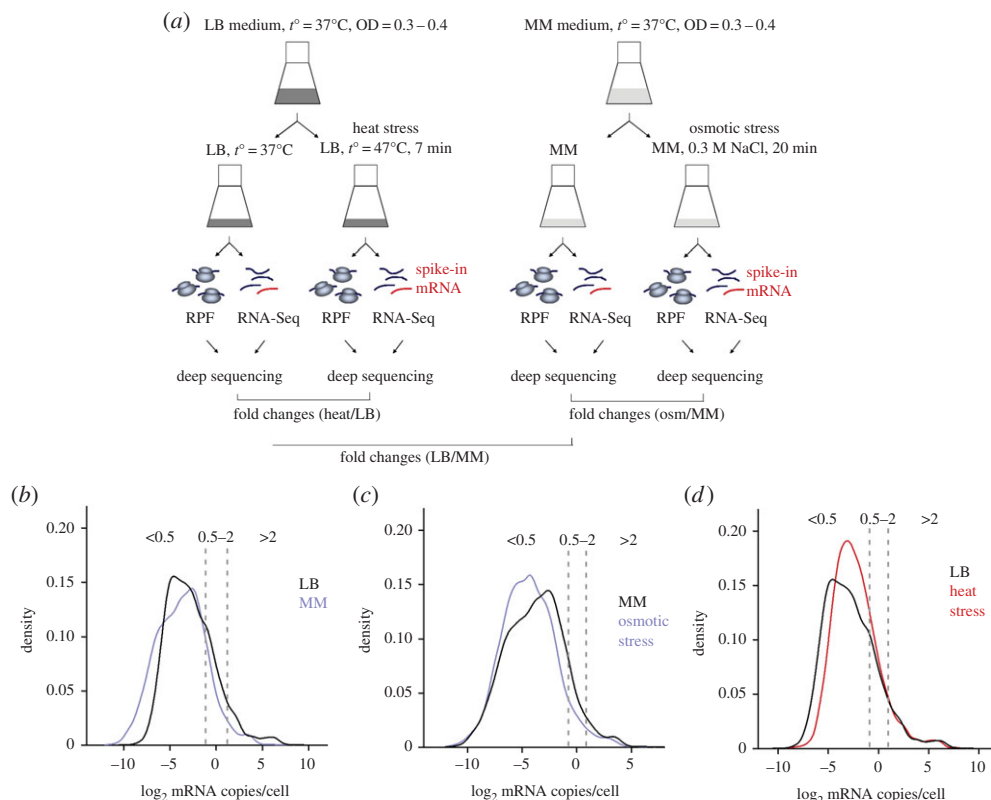


Figure 1. Changes of the mRNA copy numbers upon stress. (a) Schematic of the experiment to analyse differences in expression under different stress conditions. Distribution of the gene copy numbers quantified from the RNA-Seq datasets from cells grown in MM and LB (b), exposed to osmotic (c) or heat stress (d). Dashed vertical lines delimit the three expression groups. The copy numbers between LB and MM are significantly different ($p < 0.01$ according to Kolmogorov–Smirnov test). Note the bimodal distribution evident in the LB density curve corresponding to mRNAs with large copy numbers (greater than 25).

correlating to the $4\times$ larger volume of cells cultured in LB. The mean mRNA copy number was 1.79 copies/cell in LB and 0.56 copies/cell in MM. Similar low overall mRNA copy numbers per cell have been theoretically predicted [26] and experimentally determined in ensemble and single-cell measurements for another *E. coli* strain [27]. Relatively low mRNA copies/cell have been reported also for budding [28] and fission [29] yeast; yet the unicellular eukaryotes have on average an order of magnitude higher number of total mRNA molecules per cell which mirrors the larger cell volume and larger size of their genomes compared with *E. coli*.

We separated the genes in three groups, similar to the expression zones arbitrarily defined in unicellular eukaryotic organism, fission yeast [29]: group 1 contains genes with low-abundance mRNA (less than 0.5 copies/cell); group 2 consists of genes expressed at approximately 1 mRNA copy/cell (0.5–2 copies/cell) and group 3 comprises genes with robust expression at greater than 2 mRNA copies/cell (figure 1b). In general, despite the difference in the total mRNA copy number between LB and MM, similar functional categories (GO terms) were enriched for genes expressed at greater than 2 mRNA copies/cell, whereas there was no significant GO term overlap for genes expressed at approximately 1 mRNA copy/cell (electronic supplementary material figure S1d). The high copy number group (greater than 2 copies/cell) in both LB and MM is dominated by mRNAs encoding proteins involved in translation, main metabolism pathways and adenosine triphosphate (ATP) synthesis (electronic supplementary material figure S1d). Moreover, in LB medium a subset of mRNAs is expressed at comparatively very high copy numbers giving rise

to a bimodal distribution of the transcript copy numbers (electronic supplementary material figure S1d); this subset of genes is comprised mostly of such encoding proteins participating in ribosome biogenesis and translation. The mRNAs of the ribosomal proteins were also among the transcripts with the highest mRNA copies in MM, yet their mRNA copy numbers were five to eight times lower than in LB, correlating with the much lower number of ribosomes per cell for bacteria grown in MM [30]. The second group of genes expressed at approximately 1 mRNA copy/cell (0.5–2 mRNA copies/cell) in MM comprises mostly genes involved in the production or conversion of products that are not supplied by the MM growth medium, including amino acids and nucleotides.

The group of the genes expressed at a level below one copy per cell on average is the largest group in both media (figure 1b) which could result from a small transcription rate [31] or short lifetime of a transcript [32,33]. Our results are consistent with recent sequencing experiments from fission yeast [29] or metazoan [31] which also detected a large fraction of mRNAs expressed below 1 mRNA copy/cell.

RPF-Seq revealed the position of the translating ribosomes (figure 1a) and enabled quantification of actively translated transcripts. As a quantitative measure of translation of each gene we determined the RD per gene which is defined as the ratio of the normalized RPF reads to the normalized mRNA reads for each gene (equation (2.2)). For the majority of translationally active genes (i.e. for those which RPFs were detected), the mRNA counts are positively correlated with the corresponding RPF counts (Spearman's correlation coefficients 0.89 for LB and 0.91 for MM).

Next, we compared the changes in the gene expression at the level of transcription and translation between LB and MM by assessing the \log_2 -fold changes of the mRNA counts and RD values. This analysis revealed that 605 genes were significantly (greater than 95% confidence) transcriptionally regulated (electronic supplementary material, table S1 and figure S1b). Genes participating in translation, ribosome biogenesis and aerobic respiration were enriched among the transcriptionally controlled genes (Benjamini & Hochberg corrected $p < 0.001$, electronic supplementary material, table S1). Two hundred and thirty-nine genes showed significant changes in RD values (95% confidence, electronic supplementary material, figure S1c) without any significant changes in the mRNA counts (electronic supplementary material, table S1). Interestingly, comparing the cells grown in LB with those cells grown in MM, the mRNA coverage for the majority of factors participating in translation was within the 5th percentile and RD values were not significantly changed. In other words, the RPFs increased proportionally to the mRNA reads keeping the RD values unchanged (electronic supplementary material, table S1), implying similar biosynthetic activities per unit cell volume in both LB and MM.

(b) Similarities and dissimilarities of the response programmes to counterbalance various types of acute stress

Next, we evaluated stress-induced reprogramming of gene expression at the level of transcription and translation upon exposure of the cells to two types of acute stress: *E. coli*, grown in LB or MM until the early exponential phase, were subjected to temperature shift or exposed to osmotic upshift by adding NaCl to the medium, respectively (figure 1a). The experimental conditions were chosen to allow for monitoring of rapid changes in the transcriptional and translational programmes during the acute stress response, but not to capture long-term adaptive stress reactions. The different types of stress were applied on different time scales and in different media. Thermal stress was applied for 7 min, the time at which transcription of the heat-shock induced genes is maximal [34]. Osmotic stress was applied in a time window which is prior to the onset of intrinsic osmolyte synthesis [35] and in MM which was free of any osmoprotective substances that can be taken up to counteract osmotic stress [36]. The mRNA expression of marker genes, known to be specifically upregulated in heat [5] or osmotic stress [37], was verified with quantitative RT-PCR (electronic supplementary material, figure S2a,b). Intriguingly, osmotic stress

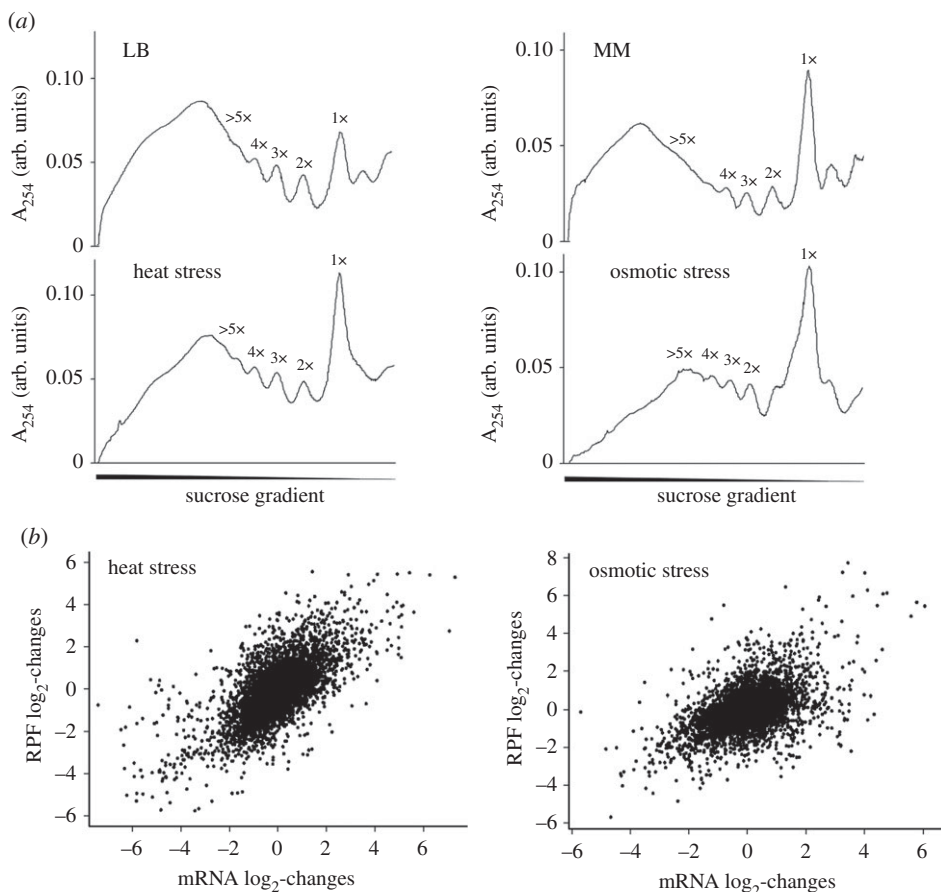


Figure 2. Transcriptional and translational response to different types of stress. (a) Polysomal profiles of cells grown in different conditions. The profiles changed for cells exposed to stress (compare LB with heat stress and MM with osmotic stress): the peaks corresponding to large polysomes decrease under stress, while the monosomal fraction (1x) increases. The fractions corresponding to mRNA with di-, tri-, tetra- and polysomes are designated as 2x, 3x, 4x and greater than 5x, respectively. (b) Correlation between the log₂-fold changes of the normalized RPF and mRNA read counts from cells exposed to heat or osmotic stress. Pearson's correlation coefficients are 0.667 (heat stress) and 0.492 (osmotic stress).

caused a global reduction of transcripts (figure 1c; electronic supplementary material, figure S2c), from approximately 2400 mRNA copies/cell in MM to approximately 1600 mRNA copies/cell upon osmotic upshift. In particular, mRNAs with higher copies (from the groups of mRNAs with greater than 2 copies/cell) were reduced (figure 1c; electronic supplementary material, figure S2e). Conversely, heat stress caused a little global reduction of the transcripts—from approximately 7800 mRNA copies/cell in LB to approximately 7200 mRNA copies/cell (figure 1d; electronic supplementary material, figure S2d,e).

To assess the global effect of stress on translation, we compared the polysome profiles under stress with the corresponding control condition (figure 2a). In both types of stress, the amount of the large polysome fraction (greater than 5 ribosomes) decreased in parallel to the increase of the monosome peak (figure 2a) which is likely a result of ribosomal drop-off [38] and implies a general repression of translation. Yet, some translation activity is retained as evidenced by the presence of 2- to 5-polysomes (figure 2a). We then compared the mRNA and RPF counts for each gene under both stress conditions (figure 2b). Overall, for the majority of translationally

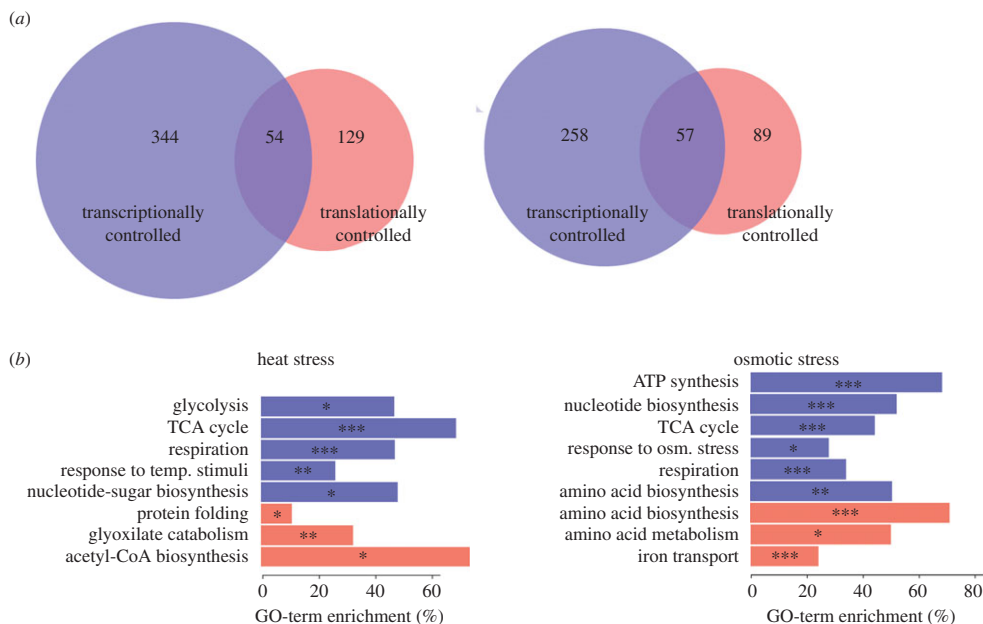


Figure 3. Fold-change analysis of the cellular response to stress. (a) Venn diagram showing the genes differentially expressed between heat stress versus LB and osmotic stress versus MM. Transcriptionally controlled, genes with mRNA (read counts) \log_2 -fold changes over the 95th percentile threshold of biological replicates (electronic supplementary material, figure S1b); translationally controlled, genes with RD \log_2 -fold changes over the 95th percentile threshold of biological replicates (electronic supplementary material, figure S1c); overlap, genes with significant changes in both mRNA and RD values. The genes in each diagram correspond to the genes listed in electronic supplementary material, table S1. (b) GO terms with significant enrichment under heat stress versus LB and under osmotic stress versus MM. The colour code is the same as in (a). *** $p < 0.001$, ** $p < 0.01$; * $p < 0.05$.

active genes under stress (i.e. for which RPFs were detected), we found that the log-log linear correlation between the mRNA and RPF changes is relatively high and positive for both stress conditions (figure 2b). On a global scale, we observed that changes in mRNA counts are co-directional with changes in the RPF counts, for both induced and repressed genes, in response to heat or osmotic stress, with correlation coefficients of 0.667 or 0.492, respectively (figure 2b). However, for both stress conditions, a sizeable fraction of genes oppose this trend: for these genes, changes in mRNA counts do not correlate with changes of the RPF counts. This raised the question as to whether these gene sets shape the cellular response against each type of stress. To compare expression between different conditions, we performed pairwise comparison of RD and mRNA read counts and ranked them according to the \log_2 -fold changes (figure 3a; electronic supplementary material, table S1). Comparison of the gene groups with significant changes upon osmotic upshift and heat exposure (greater than 95% confidence from the biological replicates, electronic supplementary material, figure S1b,c) revealed a common pattern in the response to both types of stress: 43.3% of the genes showed similar \log_2 -fold changes at transcriptional level, while only 15.7% displayed similarities of their fold changes at the level of translation, as captured by the RD values (electronic supplementary material, table S1). When mammalian cells are exposed to thermal stress, RPFs accumulate within the first 30–40 nt at the start of the genes [39,40].

In bacteria, subunits alternative to the housekeeping σ^{70} (*rpoD*)-factor of the RNA polymerase orchestrate the expression of stress-related genes to counteract external stress [41]. The mRNA levels of σ^{32} (*rpoH*, related to heat stress) were upregulated under both osmotic and thermal stress, while σ^S (*rpoS*, related to starvation stress) and σ^E (*rpoE*, related to periplasmic stress) were

upregulated only under osmotic upshift (electronic supplementary material, table S1). Despite the pervasive upregulation of transcription of *rpoH* under both osmotic and thermal stress condition, the downstream genes of the heat-shock regulon (chaperones, proteases of the Clp-family [42]), whose expression is regulated by σ^{32} [42], were upregulated only at elevated temperature with \log_2 -fold changes in the mRNA coverage ranging from 1.6 to 6.3 (e.g. *dnaK*—5.6, *dnaJ*—5.1, *clpB*—6.3, *clpX*—1.9, *clpP*—1.8) (figure 3; electronic supplementary material, table S1). The specific expression of some marker genes, specifically upregulated in heat stress [5], was verified with quantitative RT-PCR (electronic supplementary material, figure S2a). Notably, under the heat stress, the translation of the genes from the heat-shock regulon was also enhanced, i.e. the absolute number of RPFs was higher under heat stress, though the overall RD ratio remained similar to LB. Upon exposure to osmotic stress, we did not detect any upregulation of genes from the heat regulon other than *clpB* (fold-change 1.89), implying the high specificity of σ^{32} -dependent regulation under heat stress.

(c) Genes with lower secondary structure propensity are translated under thermal stress

Bacteria use complex strategies to coordinate temperature-dependent expression, including temperature-sensing RNA sequences—RNA thermometers—whose structure melts at elevated growth temperature and increases the efficiency of translation initiation [43]. Next, we compared the expression of two established examples of translational regulation in *E. coli*, *rpoH* and *ibpA* [43], using our genome-wide analysis under heat stress. For both genes, the absolute number of RPFs increased significantly under heat stress, although the RD for *ibpA* increased while for *rpoH* it remained similar to the unstressed condition because of corresponding changes of *rpoH* mRNAs (electronic supplementary material, table S1). The cellular concentration of σ^{32} at elevated temperature is comprehensively balanced at different levels, including transcriptional, translational and post-translational protein stabilization [43–45]. Importantly, the RPF reads for both genes did not change under osmotic stress.

In addition to the genes regulated by the σ^{32} factor under heat stress, 94 of the 129 genes exhibited a significant boost in translation (positive fold-change of RD) without any changes in the mRNA read counts (figure 3a; electronic supplementary material, table S1). This group was mostly enriched with genes participating in protein folding ($p < 0.01$) and metabolic activities ($p < 0.01$ and $p < 0.05$; figure 3b). The transcripts of these genes were highly translated, with high RPF coverage along the whole mRNA and no significant accumulation of reads in the 5'-region of the ORFs as in the all-genes group (figure 4a). We hypothesized that this gene set might bear some structural features to facilitate translation and thus we calculated the folding energy in the sequences flanking the initiation start. Typically, the folding profiles of all genes (figure 4b, black line) showed reduced folding stability and fewer paired nucleotides around the initiation start compared with the coding sequence (observed as a peak in the folding energy profile) [24]. The folding energy of the genes translationally upregulated under heat was significantly lower than that of the remaining genes in the genome not only around the initiation site but also over much broader sequences flanking the initiation (figure 4b). Their folding energy is significantly different from that of randomly sampled genes (grey shadowed area, $p = 0.00204$, figure 4b). 5'-UTRs, which tend to be less structured than the protein-coding sequence of the gene [24], were also less structured in the translationally upregulated genes under heat stress (figure 4b). Further downstream of the start codon, along the coding mRNA sequence, the folding energy relaxes to the mean folding profile of all genes (electronic supplementary material, figure S3a). Reduced mRNA secondary structure around the start codon facilitates expression [24,46,47] and analysis of the mRNA folding stability at the initiation start revealed a positive correlation with the changes in the RD values under heat stress; lower folding stability correlated with higher changes of the RD values (electronic supplementary material, figure S3b). Interestingly, genes whose translation is favoured under heat stress do not originate solely from the subgroup with the least structured initiation area (1–500 gene group, electronic supplementary material, figure S3b); rather these

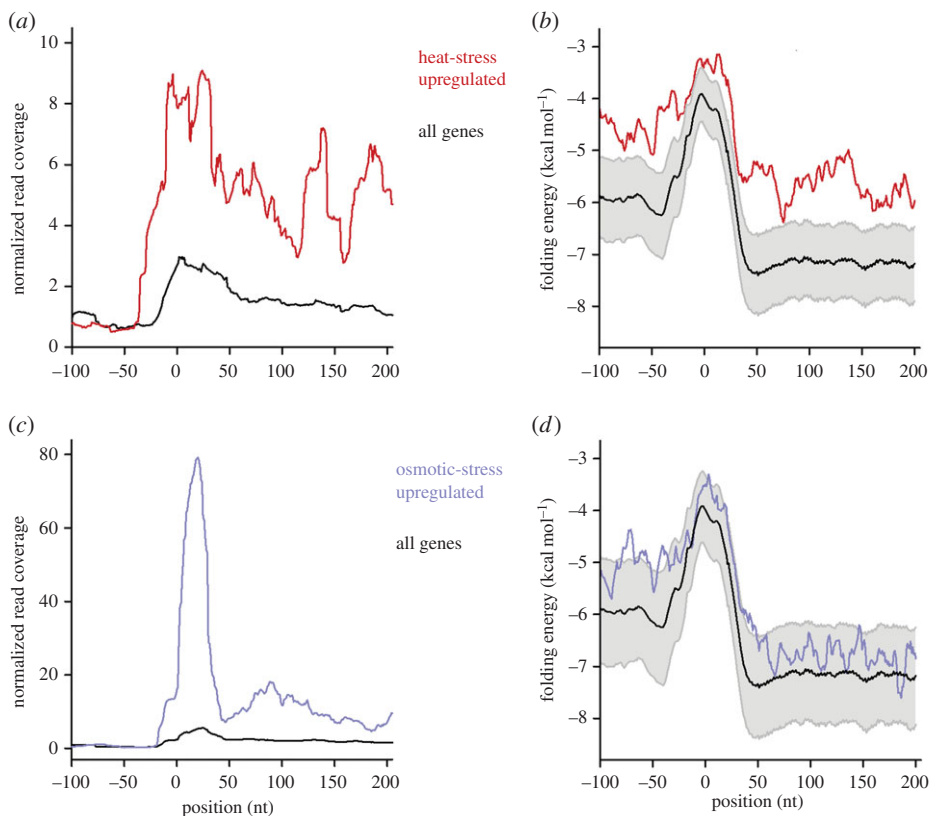


Figure 4. Genes translationally upregulated under heat stress have much lower propensity to form secondary structure. Normalized read coverage for upregulated genes under heat (red line) (a) and osmotic (blue line) (c) stresses. The RPF reads for all genes in each group were normalized to the median of the corresponding mRNA reads and aligned at the start (zero is the first nucleotide of the start codon in each ORF) and compared with all genes (black lines in a and c). Average folding energy of upregulated genes under heat (red line) (b) and upon exposure to osmotic stress (blue line) (d) compared with all protein-coding genes in *E. coli* (black lines in b and d). *p*-values (median averaged from a two-sample Kolmogorov–Smirnov test) for the upregulated genes under heat (b) 0.00204 (lower quartile: 0.00027; upper quartile: 0.01434) and osmotic stress (d) 0.58343 (lower quartile: 0.42999; upper quartile: 0.57026). The area of folding energy distribution sampled from random gene groups of the same size (as the upregulated gene group) is shadowed in grey (b and d). *p*-values from the sampling for genes under heat (b) and osmotic (d) stress are 0.0014 and 0.26072, respectively.

upregulated genes contain genes from subgroups with various folding energies, including the group with the most structured initiation region.

In *E. coli*, a large fraction (53%) of protein-coding genes is organized in operons as polycistronic mRNAs and is suggested to coordinate the expression of functionally related proteins [48]. Among the genes translationally upregulated under heat stress those residing in operons were significantly less than the genome-wide operon configuration of *E. coli* (45% versus 53%, $p = 9.36 \times 10^{-6}$). Furthermore, even for the few of them encoded within the same polycistronic mRNA we did not detect a coordinated expression. This might be not surprising in light of the fact that translation levels of ORFs within the same polycistronic mRNA largely differ as they underlie independent initiation [49] and the strength of the Shine–Dalgarno (SD) sequence differs between the ORFs within one operon [50].

Together, this implies that the response to acute heat stress is at least in part shaped by selection of a subset of genes whose structure up- and downstream of the translation start most likely undergoes significant melting at higher temperatures. Thus, the initiation regions of these genes become more accessible upon heat stress, facilitating ribosome binding and, in turn, translation.

(d) Under osmotic upshift cells reallocate translation resources

Exposure of *E. coli* to high osmolarity causes rapid loss of water (plasmolysis), turgor pressure and shrinkage of the cell. A crucial reaction of the cell is the upregulation of osmotic stress-protective genes and genes encoding ATP-driven transporters of ions and small solutes [36,51]. Their expression was mainly regulated at the level of transcription with significant increase of the mRNA copy numbers (figure 3a; electronic supplementary material, table S1); the RPFs increased proportionally to the mRNA reads while the RD values remained unchanged. The major transporters maintaining the uptake of osmotic substances, *proV*, *proP*, *proX*, *proW*, *otsA*, under osmotic upshift were expressed at very high copy numbers (greater than 2 mRNA copies/cell); by contrast, their copy numbers were extremely low in MM, less than 0.5 mRNA copies/cell. The mRNA expression of those marker genes, known to be specifically upregulated under osmotic stress [37], was verified with quantitative RT-PCR (electronic supplementary material, figure S2b).

The cell response to osmotic stress at the translational level was clearly distinct from the response to acute heat stress: different sets of genes maintain the cell response at the level of translation, i.e. genes with significant \log_2 -changes of the RD values but invariant mRNA read counts. The group of translationally upregulated genes under osmotic stress was enriched for transcripts of genes participating in amino acid metabolic processes ($p < 0.05$) and iron transport ($p < 0.001$; figure 3b). Although those genes do share some functional similarities they were not enriched in genes encoded by the same polycistronic mRNA ($p = 0.26$ compared with the genome-wide fraction of genes organized in operons).

Next, we analysed the cumulative profiles of this gene group (figure 4c). Upregulated genes showed much higher accumulation of RPFs in the first 30 nt and also approximately 10 nt upstream of the gene start (figure 4c). This was clearly not driven by any secondary structural features of the mRNA specific to these genes; their propensity to be involved in secondary structure was not significantly distinguishable from the profiles of the other transcripts (figure 4d). Importantly, translationally upregulated genes under osmotic stress also show higher accumulation of RPFs upstream of the start codon in the vicinity of the SD sequence which raised the question as to whether those genes are enriched in strong SD motifs which will favour their initiation. We performed a search for SD motifs based on the minimum hybridization energy as described in [50]; however, SD sequences were not significantly enriched in those genes ($p = 0.025$).

Osmotic stress, but not thermal stress, resulted in a 35% reduction of the mRNA transcripts globally, whereby transcripts with high copy numbers in normal conditions (greater than 2 mRNA copies/cell) were the most affected (figure 1c; electronic supplementary material, figure S2c). Over 25% of the genes in the high copy number group had significantly reduced transcripts (electronic supplementary material, figure S2e). The subset of the genes with greater than 2 mRNA copies/cell which underwent reduction in their copy numbers upon osmotic stress were also highly translated (electronic supplementary material, figure S1f), implying that the reduction of these abundant, highly translated transcripts will release a large portion of ribosomes.

4. Discussion

Here, we quantify mRNA abundance and translational activities of *E. coli* using deep sequencing of RPFs. Even though *E. coli* is an extensively studied organism, the response to different types of acute stress has a complexity not captured by existing studies. A small subset of genes, unique for each type of stress, is regulated only at the level of translation, while the majority of translationally active genes show concordant co-directional changes between mRNA and translation (RPF). A common feature among the genes translationally upregulated under heat stress is their higher accessibility in the initiation region at higher temperature which in turn facilitates their translation. In general, the genes from this subset are not necessarily genes with the lowest propensity to form secondary structure; some of the genes may undergo the most significant melting at elevated temperatures.

By contrast, preferential expression of genes to counterbalance osmotic stress is driven by reduction of highly abundant and highly translated transcripts, thereby making translation resources available to the whole pool of mRNAs which contains mRNAs that remained intact under stress or newly synthesized mRNAs. Under normal conditions more than 90% of the ribosomes are involved in translation [52,53] thus leaving little capacity to reallocate ribosomes to new mRNAs [54]. Upon exposure to osmotic stress the global transcript level is reduced significantly, by about 33% (from approximately 2400 mRNA copies/cell in MM to approximately 1600 mRNA copies/cell), thereby preferably highly translated mRNAs with high copy numbers are significantly reduced. As the number of ribosomes does not change during osmotic stress, as estimated for yeast, the hypothesis that transcript reduction is linked to re-distribution of translational capacity is supported by a theoretical study suggesting that in *E. coli* continuous growth rate and nutrient quality are balanced by the ribosome allocation [55]. Moreover, transcript reduction was also observed by exposure of yeast to osmotic upshift [56] implying conserved features of response across the species. The effect of transcript reduction is highly specific for osmotic stress: the transcript reduction upon heat exposure is 7.6% (from approx. 7800 mRNA copies/cell in LB to approx. 7200 mRNA copies/cell).

The five major transporters maintaining the uptake of osmotic substances, *proV*, *proP*, *proX*, *proW*, *otsA*, were expressed at normal conditions at very low copy number less than 0.5 copies/cell are upregulated to greater than 2 copies/cell upon osmotic upshift. Other osmotic stress-related genes are upregulated from approximately 1 mRNA copy/cell in MM to greater than 2 copies/cell upon osmotic stress. Under normal conditions their translation will compete with genes involved in key physiological processes, translation and energy metabolism (expressed at greater than 2 copies/cell). Thus, the reduction of the total amount of mRNA serves to replenish the pool of free ribosomes, which in turn boosts the translation on the remaining pool of mRNAs.

Ultimately, proteins mediate stress response and their levels have to be rapidly adjusted to ensure cell adaptability and survival under stress. Our observations are in a qualitative agreement with an earlier observation suggesting that the average copy number correlates well with the average protein concentration [27]. Previous analysis comparing transcript and protein abundance in *E. coli* concluded a relatively good correlation on a global, population level, while on a single-cell level, the mRNA and protein levels correlate poorly. This poor correlation is often attributed to different time scales of transcript and protein turnover [27]. Although each RPF read on an mRNA is producing a protein [49], the RPF coverage does not give information on protein amounts, and thus we cannot judge the contribution of protein degradation.

In summary, our data reveal a multifaceted stress-specific response in bacteria towards acute thermal and osmotic stress, enabled by a versatile induction of transcriptional and translational programmes. Unicellular organisms lack the internal homeostatic buffering capacity of multicellular species, and for survival under acute stress they need a quick reprogramming of their cellular activities. For the majority of genes, changes in the mRNA level correspond to the translation level for both types of stress. Outside of these genes, a unique fraction of genes are regulated only at the level of translation in response to the two stress conditions we studied. Indeed, reprogramming of cellular activities by translating existing mRNAs is more efficient than the response shaped by de novo transcription followed by translation enabling the cell to respond faster to changing environments.

Data accessibility. The sequencing data have been submitted to Gene Express Omnibus (GEO; GSE68762) database.

Authors' contributions. I.F. performed all ribosome profiling and deep-sequencing experiments. A.B. and P.F. analysed the sequencing data and contributed to data interpretation. G.Z. mapped the sequencing data; A.V. and C.S. contributed to the fold-change analysis. I.F. and Z.I. conceived concepts, planned and designed the experiments, and Z.I. and A.B. wrote the manuscript.

Competing interests. We declare we have no competing interests.

Funding. This work was supported by grants of the Deutsche Forschungsgemeinschaft (to Z.I.) and European Union (ITN NICHE) (to Z.I. and A.V.).

Acknowledgements. We thank Wei Chen and Mirjam Feldkamp (Max Delbrück Center, Berlin) for assistance with the sequencing.

References

- de Nadal E, Ammerer G, Posas F. 2011 Controlling gene expression in response to stress. *Nat. Rev. Genet.* **12**, 833–845. (doi:10.1038/nrg3055)
- Akerfelt M, Morimoto RI, Sistonen L. 2010 Heat shock factors: integrators of cell stress, development and lifespan. *Nat. Rev. Mol. Cell Biol.* **11**, 545–555. (doi:10.1038/nrm2938)
- Gunasekera TS, Csonka LN, Paliy O. 2008 Genome-wide transcriptional responses of *Escherichia coli* K-12 to continuous osmotic and heat stresses. *J. Bacteriol.* **190**, 3712–3720. (doi:10.1128/JB.01990-07)
- Lopez-Maury L, Marguerat S, Bahler J. 2008 Tuning gene expression to changing environments: from rapid responses to evolutionary adaptation. *Nat. Rev. Genet.* **9**, 583–593. (doi:10.1038/nrg2398)
- Richter K, Haslbeck M, Buchner J. 2010 The heat shock response: life on the verge of death. *Mol. Cell* **40**, 253–266. (doi:10.1016/j.molcel.2010.10.006)
- Ideker T *et al.* 2001 Integrated genomic and proteomic analyses of a systematically perturbed metabolic network. *Science* **292**, 929–934. (doi:10.1126/science.292.5518.929)
- Komili S, Silver PA. 2008 Coupling and coordination in gene expression processes: a systems biology view. *Nat. Rev. Genet.* **9**, 38–48. (doi:10.1038/nrg2223)
- Vogel C, Marcotte EM. 2012 Insights into the regulation of protein abundance from proteomic and transcriptomic analyses. *Nat. Rev. Genet.* **13**, 227–232. (doi:10.1038/nrg3185)
- Belasco JG. 2010 All things must pass: contrasts and commonalities in eukaryotic and bacterial mRNA decay. *Nat. Rev. Mol. Cell Biol.* **11**, 467–478. (doi:10.1038/nrm2917)
- Ingolia NT, Ghaemmhami S, Newman JR, Weissman JS. 2009 Genome-wide analysis *in vivo* of translation with nucleotide resolution using ribosome profiling. *Science* **324**, 218–223. (doi:10.1126/science.1168978)
- Li GW, Oh E, Weissman JS. 2012 The anti-Shine–Dalgarno sequence drives translational pausing and codon choice in bacteria. *Nature* **484**, 538–541. (doi:10.1038/nature10965)
- Oh E *et al.* 2011 Selective ribosome profiling reveals the cotranslational chaperone action of trigger factor *in vivo*. *Cell* **147**, 1295–1308. (doi:10.1016/j.cell.2011.10.044)
- Cozzzone AJ, Stent GS. 1973 Movement of ribosomes over messenger RNA in polysomes of *rel⁺* and *rel⁻* *Escherichia coli* strains. *J. Mol. Biol.* **76**, 163–179. (doi:10.1016/0022-2836(73)90087-9)
- Guo H, Ingolia NT, Weissman JS, Bartel DP. 2010 Mammalian microRNAs predominantly act to decrease target mRNA levels. *Nature* **466**, 835–840. (doi:10.1038/nature09267)
- He S *et al.* 2010 Validation of two ribosomal RNA removal methods for microbial metatranscriptomics. *Nat. Methods* **7**, 807–812. (doi:10.1038/nmeth.1507)
- Ingolia NT. 2010 Genome-wide translational profiling by ribosome footprinting. *Methods Enzymol.* **470**, 119–142. (doi:10.1016/S0076-6879(10)70006-9)
- Jiang L, Schlesinger F, Davis CA, Zhang Y, Li R, Salit M, Gingeras TR, Oliver B. 2011 Synthetic spike-in standards for RNA-seq experiments. *Genome Res.* **21**, 1543–1551. (doi:10.1101/gr.121095.111)
- Zhang G, Fedyunin I, Kirchner S, Xiao C, Valleriani A, Ignatova Z. 2012 FANSe: an accurate algorithm for quantitative mapping of large scale sequencing reads. *Nucleic Acids Res.* **40**, e83. (doi:10.1093/nar/gks196)
- Mortazavi A, Williams BA, McCue K, Schaeffer L, Wold B. 2008 Mapping and quantifying mammalian transcriptomes by RNA-Seq. *Nat. Methods* **5**, 621–628. (doi:10.1038/nmeth.1226)
- Dillies MA *et al.* 2012 A comprehensive evaluation of normalization methods for Illumina high-throughput RNA sequencing data analysis. *Brief. Bioinform.* **14**, 671–683. (doi:10.1093/bib/bbs046)
- Bullard JH, Purdom E, Hansen KD, Dudoit S. 2010 Evaluation of statistical methods for normalization and differential expression in mRNA-Seq experiments. *BMC Bioinform.* **11**, 94. (doi:10.1186/1471-2105-11-94)
- Benjamini Y, Hochberg Y. 1995 Controlling the false discovery rate: a practical and powerful approach to multiple testing. *J. R. Stat. Soc. B* **57**, 289–300.

23. Lorenz R, Bernhart SH, Honer Zu Siederdisen C, Tafer H, Flamm C, Stadler PF, Hofacker IL. 2011 ViennaRNA Package 2.0. *Algorithms Mol. Biol.* **6**, 26. (doi:10.1186/1748-7188-6-26)
24. Bentele K, Saffert P, Rauscher R, Ignatova Z, Blüthgen N. 2013 Efficient translation initiation dictates codon usage at gene start. *Mol. Syst. Biol.* **9**, 675. (doi:10.1038/msb.2013.32)
25. Scharff LB, Childs L, Walther D, Bock R. 2011 Local absence of secondary structure permits translation of mRNAs that lack ribosome-binding sites. *PLoS Genet.* **7**, e1002155. (doi:10.1371/journal.pgen.1002155)
26. Bremer H, Dennis P, Ehrenberg M. 2003 Free RNA polymerase and modeling global transcription in *Escherichia coli*. *Biochimie* **85**, 597–609. (doi:10.1016/S0300-9084(03)00105-6)
27. Taniguchi Y, Choi PJ, Li GW, Chen H, Babu M, Hearn J, Emili A, Xie XS. 2010 Quantifying *E. coli* proteome and transcriptome with single-molecule sensitivity in single cells. *Science* **329**, 533–538. (doi:10.1126/science.1188308)
28. Zenklusen D, Larson DR, Singer RH. 2008 Single-RNA counting reveals alternative modes of gene expression in yeast. *Nat. Struct. Mol. Biol.* **15**, 1263–1271. (doi:10.1038/nsmb.1514)
29. Marguerat S, Schmidt A, Codlin S, Chen W, Aebersold R, Bahler J. 2012 Quantitative analysis of fission yeast transcriptomes and proteomes in proliferating and quiescent cells. *Cell* **151**, 671–683. (doi:10.1016/j.cell.2012.09.019)
30. Tao H, Bausch C, Richmond C, Blattner FR, Conway T. 1999 Functional genomics: expression analysis of *Escherichia coli* growing on minimal and rich media. *J. Bacteriol.* **181**, 6425–6440.
31. Hebenstreit D, Fang M, Gu M, Charoensawan V, van Oudenaarden A, Teichmann SA. 2011 RNA sequencing reveals two major classes of gene expression levels in metazoan cells. *Mol. Syst. Biol.* **7**, 497. (doi:10.1038/msb.2011.28)
32. Deneke C, Lipowsky R, Valleriani A. 2013 Complex degradation processes lead to non-exponential decay patterns and age-dependent decay rates of messenger RNA. *PLoS ONE* **8**, e55442. (doi:10.1371/journal.pone.0055442)
33. Deneke C, Rudolf S, Valleriani A. 2012 Transient phenomena in gene expression after induction of transcription. *PLoS ONE* **7**, e35044. (doi:10.1371/journal.pone.0035044)
34. Guisbert E, Yura T, Rhodius VA, Gross CA. 2008 Convergence of molecular, modeling, and systems approaches for an understanding of the *Escherichia coli* heat shock response. *Microbiol. Mol. Biol. Rev.* **72**, 545–554. (doi:10.1128/MMBR.00007-08)
35. Booth IR, Cairney J, Sutherland L, Higgin CF. 1988 Enteric bacteria and osmotic stress: an integrated homeostatic system. *Soc. Appl. Bacteriol. Symp. Ser.* **17**, 35S–49S. (doi:10.1111/j.1365-2672.1988.tb04463.x)
36. Wood JM, Bremer E, Csonka LN, Kraemer R, Poolman B, van der Heide T, Smith LT. 2001 Osmosensing and osmoregulatory compatible solute accumulation by bacteria. *Comp. Biochem. Physiol. A Mol. Integr. Physiol.* **130**, 437–460. (doi:10.1016/S1095-6433(01)00442-1)
37. Weber A, Jung K. 2002 Profiling early osmostress-dependent gene expression in *Escherichia coli* using DNA microarrays. *J. Bacteriol.* **184**, 5502–5507. (doi:10.1128/JB.184.19.5502-5507.2002)
38. Zhang G, Fedyunin I, Miekley O, Valleriani A, Moura A, Ignatova Z. 2010 Global and local depletion of ternary complex limits translational elongation. *Nucleic Acids Res.* **38**, 4778–4787. (doi:10.1093/nar/gkq196)
39. Liu B, Han Y, Qian SB. 2013 Cotranslational response to proteotoxic stress by elongation pausing of ribosomes. *Mol. Cell* **49**, 453–463. (doi:10.1016/j.molcel.2012.12.001)
40. Shalgi R, Hurt JA, Krykbaeva I, Taipale M, Lindquist S, Burge CB. 2013 Widespread regulation of translation by elongation pausing in heat shock. *Mol. Cell* **49**, 439–452. (doi:10.1016/j.molcel.2012.11.028)
41. Mooney RA, Darst SA, Landick R. 2005 Sigma and RNA polymerase: an on-again, off-again relationship? *Mol. Cell* **20**, 335–345. (doi:10.1016/j.molcel.2005.10.015)
42. Mogk A, Huber D, Bukau B. 2011 Integrating protein homeostasis strategies in prokaryotes. *Cold Spring Harb. Perspect. Biol.* **3**, a004366. (doi:10.1101/cshperspect.a004366)
43. Kortmann J, Narberhaus F. 2012 Bacterial RNA thermometers: molecular zippers and switches. *Nat. Rev. Microbiol.* **10**, 255–265. (doi:10.1038/nrmicro2730)
44. Arsene F, Tomoyasu T, Bukau B. 2000 The heat shock response of *Escherichia coli*. *Int. J. Food Microbiol.* **55**, 3–9. (doi:10.1016/S0168-1605(00)00206-3)
45. Erickson JW, Gross CA. 1989 Identification of the sigma E subunit of *Escherichia coli* RNA polymerase: a second alternate sigma factor involved in high-temperature gene expression. *Genes Dev.* **3**, 1462–1471. (doi:10.1101/gad.3.9.1462)

46. Goodman DB, Church GM, Kosuri S. 2013 Causes and effects of N-terminal codon bias in bacterial genes. *Science* **342**, 475–479. (doi:10.1126/science.1241934)
47. Kudla G, Murray AW, Tollervey D, Plotkin JB. 2009 Coding-sequence determinants of gene expression in *Escherichia coli*. *Science* **324**, 255–258. (doi:10.1126/science.1170160)
48. Jackson RJ, Kaminski A, Pöyry TAA. 2007 Coupled termination-reinitiation events in mRNA translation. In *Translational control in biology and medicine* (eds MB Matthews, N Sonenberg, JWB Hurshey), pp. 197–223. New York, NY: Cold Spring Harbor Laboratory Press.
49. Li GW, Burkhardt D, Gross C, Weissman JS. 2014 Quantifying absolute protein synthesis rates reveals principles underlying allocation of cellular resources. *Cell* **157**, 624–635. (doi:10.1016/j.cell.2014.02.033)
50. Ma J, Campbell A, Karlin S. 2002 Correlations between Shine-Dalgarno sequences and gene features such as predicted expression levels and operon structures. *J. Bacteriol.* **184**, 5733–5745. (doi:10.1128/JB.184.20.5733-5745.2002)
51. Weber A, Kogl SA, Jung K. 2006 Time-dependent proteome alterations under osmotic stress during aerobic and anaerobic growth in *Escherichia coli*. *J. Bacteriol.* **188**, 7165–7175. (doi:10.1128/JB.00508-06)
52. Bremer H, Dennis P. 2008 Feedback control of ribosome function in *Escherichia coli*. *Biochimie* **90**, 493–499. (doi:10.1016/j.biochi.2007.10.008)
53. Warner JR, Vilardell J, Sohn JH. 2001 Economics of ribosome biosynthesis. *Cold Spring Harb. Symp. Quant. Biol.* **66**, 567–574. (doi:10.1101/sqb.2001.66.567)
54. Shah P, Ding Y, Niemczyk M, Kudla G, Plotkin JB. 2013 Rate-limiting steps in yeast protein translation. *Cell* **153**, 1589–1601. (doi:10.1016/j.cell.2013.05.049)
55. Scott M, Gunderson CW, Mateescu EM, Zhang Z, Hwa T. 2010 Interdependence of cell growth and gene expression: origins and consequences. *Science* **330**, 1099–1102. (doi:10.1126/science.1192588)
56. Lee MV, Topper SE, Hubler SL, Hose J, Wenger CD, Coon JJ, Gasch AP. 2011 A dynamic model of proteome changes reveals new roles for transcript alteration in yeast. *Mol. Syst. Biol.* **7**, 514. (doi:10.1038/msb.2011.48)